Rotational dynamics of molecular impurities in alkali halide crystals

S. D. Mahanti and P. Murray

Department of Physics, Michigan State University, East Lansing, Michigan 48824-1116

G. Kemeny

College of Natural Science, Michigan State University, East Lansing, Michigan 48824-1116

(Received 15 November 1984)

We have carefully investigated the orientational dynamics of a single substitutional diatomic molecular impurity in alkali halide crystals. The orientational relaxation functions of E_g and T_{2g} symmetries are calculated by using Mori's projection-operator technique with truncation first applied to the rigid-lattice case by de Raedt and Michel [Phys. Rev. B **19**, 767 (1979)]. For the CN^- impurity in a rigid KBr lattice we find that the librational and central-peak behaviors of the spectral weight function for the two symmetries are strongly influenced by the hexadecapole moment of the molecular ion. We find that the rotation-translation coupling modifies the single-site cubic potential by self-energy corrections, suppresses librational motion, enhances diffusive motion, and narrows the width of the central peak.

I. INTRODUCTION

Orientational structure and dynamics of simple diatomic molecular impurities in cubic host lattices have been a problem of considerable interest over the past several years.[1-6] Typical systems are $(CN)^-$ and O_2^- ions in alkali halide crystals. Recently[7] these systems, in particular $(CN)^-$ in KCl and NaCl, have been explored in great detail to understand how the structure and dynamics evolve from the single-impurity limit to the molecular-crystal limit with special focus on the orientational glass phase[8] observed in the intermediate-concentration range.

A necessary starting point for understanding the dynamic properties of the glass phase in these systems is a proper study of the single-impurity limit. This latter problem is interesting in its own right as it forms a prototype of a problem of a single molecular impurity described by its orientational degrees of freedom coupled strongly to a polarizable medium, a problem similar to the polaron problem.[9] Therefore, as in the polaron case, one expects to find here effects similar to effective-mass enhancement and self-trapping.

In this paper we discuss in detail the effect of rotation-translation coupling on the orientational dynamics of a single impurity in a cubic host. A brief report of this work has been already published.[10] The dynamics in a rigid host was studied in great detail by de Raedt and Michel[5] using the Mori projection-operator technique. We have examined the physical origin of one of their interesting observations regarding the relationship between the symmetry of the dynamic variable and central-peak and librational structure of the spectral function. In addition, we have analyzed the contributions of the electric quadrupole and hexadecapole moments to the single-site potential and find them to be of great importance in the quantitative understanding of the rotational dynamics.

The organization of the paper is as follows: In Sec. II, we describe the Hamiltonian for the coupled rotation-translation system. Section III briefly reviews the de Raedt and Michel approach to obtain Kubo's orientational relaxation function using Mori's projection-operator technique. The relationship between the symmetry of the dynamic variables and the low-temperature behavior of spectral weight functions for the rigid-lattice case is discussed in Sec. IV. In Sec. V, we present the results of including rotation-translation coupling on the orientational dynamics. Finally, in Sec. VI, we present our numerical results and compare theory with experiment.

II. THE HAMILTONIAN

We study the orientational relaxation of a single diatomic molecular impurity in alkali halide hosts. The Hamiltonian H for such a system is a sum of the rotational Hamiltonian H_R for the molecule of moment of inertia I in a rigid lattice, the translational Hamiltonian of the pure lattice, H_T, and the translation-rotation coupling H_{RT}, i.e.,

$$H = H_R + H_T + H_{RT} , \qquad (2.1)$$

where

$$H_R = \frac{p_\theta^2}{2I} + \frac{p_\phi^2}{2I\sin^2\theta} + V_0(\Omega) , \qquad (2.2)$$

$$H_T = \sum_{j,\mathbf{k}} \hbar\omega_{j,\mathbf{k}}(b_{j\mathbf{k}}^\dagger b_{j\mathbf{k}} + \tfrac{1}{2}) , \qquad (2.3)$$

and

$$H_{RT} = \sum_{\alpha,j,\mathbf{k}} V_{\alpha j}(\mathbf{k}) Y_\alpha(\Omega)(b_{j,\mathbf{k}} + b_{j,-\mathbf{k}}^\dagger) . \qquad (2.4)$$

In the above equations $\Omega = (\theta, \phi)$ is the spherical angle of the molecular axis, j and $\mathbf{k}$ are the polarization and wave vector of phonons and Y_α's are the five symmetry-adapted normalized spherical harmonics of order 2. The rigid-ion orientational potential V_0 consists of nearest-

neighbor repulsion terms V_R and the hexadecapole-moment—hexadecapole-field interaction terms V_{EL}, i.e.,

$$V_0 = V_R + V_{EL} \ , \tag{2.5}$$

where

$$V_R = C_1 \sum_{s=\pm 1} \sum_j e^{-C_2 |s\mathbf{d} - \mathbf{X}_j|} \tag{2.6}$$

and

$$V_{EL} = Q_4 [A_{40} P_4^0 (\cos\theta) + A_{44} P_4^4 (\cos\theta) \cos(4\phi)] \ . \tag{2.7}$$

In Eq. (2.6) C_1 and C_2 are the Born-Mayer repulsion constants, and $\mathbf{X}_j$ (R_j, Θ_j, Φ_j) is the equilibrium position of ion j in the undistorted lattice with the molecule at the origin of the coordinate system. The vector $\mathbf{d}$ (d, θ, ϕ) describes the positions of the two atoms of the molecule, $2d$ being the internuclear separation. $P_l^m (\cos\theta)$ are associated Legendre polynomials; A_{40}, A_{44} are lattice sums, such that

$$A_{40} = \sum_j \frac{q_j}{R_j^5} P_4^0 (\cos\Theta_j) = 168 A_{44} \ , \tag{2.8}$$

q_j being the charge at the jth lattice site.

The translation-rotation coupling $V_{\alpha j}(\mathbf{k})$ can be written in the form[11,12]

$$V_{\alpha j}(\mathbf{k}) = \frac{\hbar}{2\omega_{jk}} \sum_{\mu, \kappa} \frac{1}{(m_\kappa)^{1/2}} e_\mu(\kappa, \mathbf{k}j) v_{\alpha\mu}(\kappa, \mathbf{k}) \ , \tag{2.9}$$

where ω_{jk} is the frequency of the phonon of mode $(j, \mathbf{k})$ calculated from H_T, and $e_\mu(\kappa; \mathbf{k}j)$ is the μth component of the polarization vector for ion of type κ for the mode $(j, \mathbf{k})$. The coefficients $v_{\alpha\mu}(\kappa, \mathbf{k})$ have contributions both from the short-range repulsion and quadrupole-moment—electric-field-gradient interactions and are discussed in detail in Refs. 13—15.

III. KUBO'S RELAXATION FUNCTION

The dynamics of a physical quantity described by the variable $U(\theta, \phi)$ is given by Kubo's relaxation function $\Phi_+(z)$ where z is the response frequency. This has been calculated by de Raedt and Michel using Mori theory[5] and we simply give the result

$$\Phi_+(z) = \beta \langle U, U \rangle \frac{1}{z - \langle \omega^2 \rangle / [z + \Sigma_+(z)]} \ , \tag{3.1}$$

where $\beta = 1/k_B T$, $\beta \langle U, U \rangle$ is the isothermal susceptibility associated with the variable U, and $\langle \ \rangle$ is the thermal average taken over the total Hamiltonian H. The memory function $\Sigma_+(z)$ is related to the moments $\langle \omega^{2n} \rangle$ by the relation

$$\Sigma_+(z) = -\frac{1}{\langle \omega^2 \rangle} \frac{\langle \omega^4 \rangle - \langle \omega^2 \rangle^2}{z + i (\langle \omega^4 \rangle / \langle \omega^2 \rangle)^{1/2}} \ , \tag{3.2}$$

where

$$\langle \omega^{2n} \rangle = \langle U^{(n)}, U^{(n)} \rangle / \langle U, U \rangle \ . \tag{3.3}$$

In Eq. (3.3) $U^{(n)}$ is the nth time derivative of the dynamic

variable $U(\theta, \phi)$. Equation (3.2) is approximate in the sense that effects of higher moments $(n > 2)$ on the memory function have been ignored. However, as pointed out by de Raedt and de Raedt,[16] approximation (3.2) for $\Sigma_+(z)$ satisfies important spectral sum rules.

In the calculation that follows, we will express both the time Fourier transform of $\phi_+(z)$, to be denoted as $\phi_+(t)$, and the spectral function

$$S(\omega) = -\pi^{-1} \text{Im} \phi_+(\omega + i\epsilon) |_{\epsilon \to 0}$$

in units of $\beta(U; U)$. In order to distinguish between central-peak and librational characteristics of both $S(\omega)$ and $\phi_+(t)$, we isolate the three poles of $\phi_+(z)$ in the complex z plane. In their work, de Raedt and Michel[5] looked at $S(\omega)$ directly as a function of ω instead of looking at the individual components. However, we believe that interesting physical insights can be obtained by studying the amplitudes and widths of the three different peaks of the spectral function separately. Furthermore, $\phi_+(t)$ can be compared directly with the results of molecular-dynamics simulations. Taking the Fourier transform of $\phi_+(z = \omega)$ after expressing it as the sum of three poles, we find that

$$\phi_+(t) = Ae^{-\Gamma\omega_0 t} + e^{-\gamma\omega_0 t} [X \cos(\delta\omega_0 t) + Y \sin(\delta\omega_0 t)] \ . \tag{3.4}$$

Similarly for the spectral function we obtain

$$S(\omega) = \frac{1}{\pi} \left[A \frac{\Gamma\omega_0}{\omega^2 + (\Gamma\omega_0)^2} + \frac{1}{2} \left[\frac{X\gamma\omega_0 - Y(\omega + \delta\omega_0)}{(\omega + \delta\omega_0)^2 + \gamma^2\omega_0^2} \right] \right.$$
$$\left. + \frac{1}{2} \left[\frac{X\gamma\omega_0 + Y(\omega - \delta\omega_0)}{(\omega - \delta\omega_0)^2 + \gamma^2\omega_0^2} \right] \right] \ . \tag{3.5}$$

In Eqs. (3.4) and (3.5) the spectral weights A and X are

$$A = (1 + \alpha + \alpha^2 - 1/R^2)/[\alpha(1 + 2\alpha) - 1/R^2\alpha] \tag{3.6}$$

and

$$X = 1 - A \ . \tag{3.7}$$

The parameter Y is given by the equation

$$Y = [3(S_1 + S_2)A - \alpha - 1]/\sqrt{3}(S_1 - S_2) \ . \tag{3.8}$$

The parameter α appearing in the above equations is given by

$$\alpha = (S_1 + S_2 - \tfrac{1}{3}) \ , \tag{3.9}$$

where

$$S_{1,2} = [r \pm (q^3 + r^2)^{1/2}]^{1/3} \ , \tag{3.10}$$

$$r = (\tfrac{7}{54} - 1/2R^2) \tag{3.11}$$

and

$$q = \tfrac{2}{9} \ . \tag{3.12}$$

Equation (3.5) clearly brings out the three-peak nature of the spectral function and Eq. (3.4) describes the time dependence of the corresponding correlation function. The frequency scale of the dynamics is set by $\omega_0 = \langle \omega^2 \rangle^{1/2}$ and once we scale all the frequencies by ω_0,

the structure of the spectrum is completely determined by the dimensionless quantity R, where

$$R = (\langle \omega^4 \rangle / \langle \omega^2 \rangle^2)^{1/2} . \tag{3.13}$$

Thus, R is a quantity of central importance in the study of the rotational dynamics of molecular impurities. The frequency of the librational peak δ and the widths of the central and librational peaks Γ and γ (as measured in units of ω_0) are given by

$$\delta = (S_1 - S_2) R \sqrt{3}/2 , \tag{3.14}$$

$$\Gamma = (\tfrac{1}{3} - S_1 - S_2) R , \tag{3.15}$$

and

$$\gamma = (1 + S_1 + S_2) R/2 . \tag{3.16}$$

Again the three quantities δ, Γ, and γ depend only on R. Of course, the nature of the Hamiltonian H and the parameters of the Hamiltonian vis-à-vis temperature T, will determine ω_0 and R and hence the nature of the spectral response. Furthermore, ω_0 and R will also depend sensitively on the type and symmetry of the dynamic variable U that one is concerned with. It is easy to show that the spectral function $S(\omega)$ satisfies the sum rule

$$\int_{-\infty}^{+\infty} S(\omega) d\omega = A + X = 1 . \tag{3.17}$$

Before discussing the details of the Hamiltonian appropriate for molecular impurities in alkali halides and dynamical variables of different symmetries, we would like to discuss some general features of the reduced spectral response function $\omega_0 S(\omega/\omega_0) = \widetilde{S}(\varpi)$ given by

$$\widetilde{S}(\varpi) = \frac{1}{\pi} \left[A \frac{\Gamma}{\varpi^2 + \Gamma^2} + \frac{1}{2} \left[\frac{X\gamma - Y(\varpi + \delta)}{(\omega + \delta)^2 + \gamma^2} \right. \right.$$
$$\left. \left. + \frac{X\gamma + Y(\varpi - \delta)}{(\omega - \delta)^2 + \gamma^2} \right] \right] . \tag{3.18}$$

$\widetilde{S}(\varpi)$ and various parameters that determine it are only functions of R. First we note that $R \geq 1$. In Fig. 1 of Ref. 10, we have plotted X, Γ, γ, δ, and $\tan^{-1}(Y/X)$ as functions of R. In the limit $R \to 1$, which we will refer to as the oscillator or pure librational limit, $X \to 1$, $Y \to 0$, and $A \to 0$. Thus, the entire weight is transferred to $\varpi = \pm 1$ and

$$\widetilde{S}(\varpi) = \tfrac{1}{2} [\delta(\varpi - 1) + \delta(\varpi + 1)] . \tag{3.19}$$

It should be noted that the width of the central peak Γ does not vanish as $R \to 1$, but the weight in the central peak vanishes. In the other extreme limit, i.e., $R \to \infty$, which we shall refer to as the central-peak limit, $X \to 0$, $A \to 1$, and $\Gamma \to 0$. The spectral function $\widetilde{S}(\varpi)$ is a simple δ function at the origin, i.e.,

$$\widetilde{S}(\varpi) = \delta(\varpi) . \tag{3.20}$$

The values of A, X, Y, Γ, γ, and δ for $R = 1$ and $R \to \infty$ are given in Table I. The spectrum for values of $\infty > R > 1$ can have either a one-peak, two-peak, or a three-peak structure.[5] The evolution of the reduced spectrum with increasing T will be determined primarily by the T dependence of R and the actual spectral function $S(\omega)$ by the T dependence of both the scaling frequency ω_0 and R. This we discuss in the next section.

IV. SYMMETRY OF DYNAMIC VARIABLES AND LOW-TEMPERATURE BEHAVIOR OF SPECTRAL FUNCTIONS IN A RIGID CAGE

For diatomic impurities in cubic crystals the most interesting dynamic variables are properly symmetrized spherical harmonics of order 2, i.e., $U(\theta, \phi) = Y_\alpha(\theta, \phi)$, where $\alpha = 1, 2$ refer to E_g symmetry and $\alpha = 3, 4, 5$ refer to T_{2g} symmetry.[13,14] We first assume that the molecules are moving in a static cage, i.e., we assume that H_{TR} of Eq. (2.4) is equal to zero. The equations determining $\langle \omega^2 \rangle$ and $\langle \omega^4 \rangle$ for a potential of cubic symmetry $V_0(\theta, \phi)$ are given in the Appendix. The equations for the fourth moments are in a slightly different form from those given by de Raedt and Michel.[5] An extremely interesting result that was given in Refs. 1 and 5 is the following: If the parameters of $V_0(\theta, \phi)$ [see Eq. (2.5)] are such that they have minima along the [100] and its crystallographically equivalent directions, then for $T \to 0$, the spectral function of T_{2g} symmetry is dominated by oscillatory behavior, i.e., $X \approx 1$ and $A \approx 0$ and the spectral function of E_g symmetry is dominated by central-peak behavior, i.e., $A \approx 1$ and $X = 0$. If the potential minima are along [111] and equivalent directions, then the two spectral functions interchange their characteristics.

The above-mentioned behaviors of the spectral function are shown in Figs. 1 and 2. In the numerical calculations of spectral functions we have used the parameter values appropriate for a $(CN)^-$ impurity in KBr crystal and these are given in Table II. To obtain the curves for Fig.

TABLE I. The R dependence of various spectral parameters appearing for the reduced spectral response function $\widetilde{S}(\varpi)$ of Eq. (3.18), where R^2 is the ratio of fourth moment $\langle \omega^4 \rangle$ to the square of the second moment $\langle \omega^2 \rangle$. Only $R = 1$ and $R \to \infty$ limits are given.

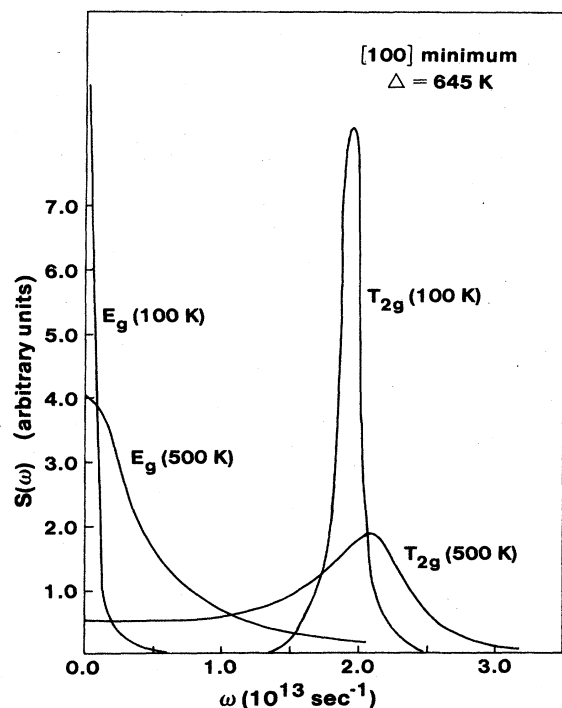|	A	X	Y	$\tan^{-1}(Y/X)$ (deg)	Γ	γ	δ
$R = 1$	0	1	0	0	1	0	1
$R \to \infty$	$1 - \dfrac{1}{R^2}$	$\dfrac{1}{R^2}$	$-\dfrac{\sqrt{3}}{R^2}$	-60	$\dfrac{1}{R}$	$\dfrac{R}{2}$	$R\dfrac{\sqrt{3}}{2}$

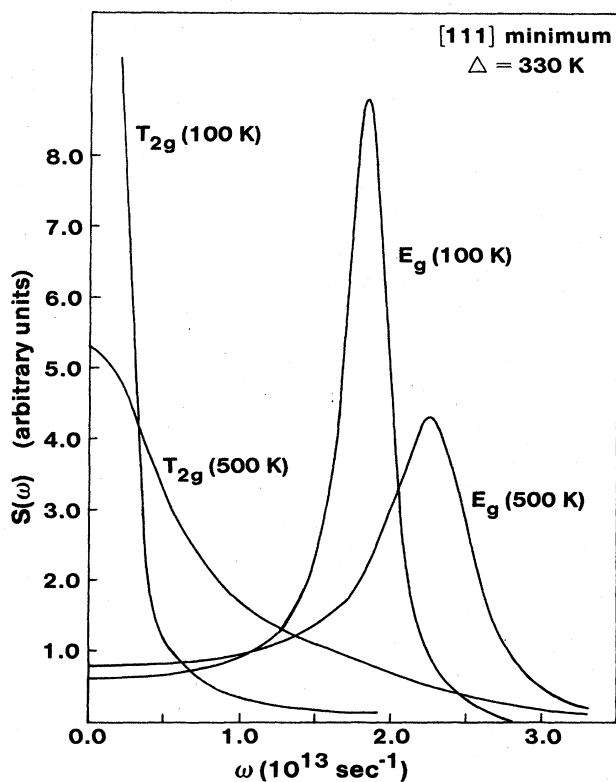FIG. 1. Frequency and temperature dependence of spectral functions for [100] minimum.

FIG. 2. Frequency and temperature dependence of spectral functions for [111] minimum.

TABLE II. Parameters for CN^- in KBr: the lattice constant $2a$, molecular size $2d$, short-range repulsive force parameters C_1 and C_2 [see Eq. (2.6)], and the electric quadrapole (Q_2) and hexadecapole (Q_4) moments of the CN^- molecular ion.

a (Å)	d (Å)	C_1 (10^7 K)	C_2 (Å^{-1})	Q_2 (a.u.)	Q_4 (a.u.)
3.25	0.60	2.347	3.3382	-3.9642[a]	-11.91[a]

[a]Free-$(CN)^-$-ion value taken from LeSar and Gordon (Ref. 16).

1, we have included both short-range repulsion and hexadecapole-moment contributions to $V_0(\theta,\phi)$. The latter dominates the former and the minima of $V_0(\theta,\phi)$ are along [100] and crystallographically equivalent directions. The results of Fig. 2 have been obtained by considering only the short-range repulsion contribution to $V_0(\theta,\phi)$. We should point out that such effects of the change in the direction of the minima of $V_0(\theta,\phi)$ can be directly observed in the Raman scattering experiments.[1]

The numerical calculations presented above suggest that the differences between E_g and T_{2g} are due to their respective behaviors at and near the potential minima. In order to examine this point we consider a harmonic oscillator with the Hamiltonian

$$H = \frac{p^2}{2m} + \frac{K}{2}\phi^2 \tag{4.1}$$

and three dynamical variables

$$A_n = n\phi, \quad B_n = 1 - \frac{n^2\phi^2}{2}, \quad C_n = -\frac{n^2\phi^2}{2}. \tag{4.2}$$

The spectral moments are

$$\langle \omega_A^2 \rangle = K/m, \tag{4.3a}$$

$$\langle \omega_B^2 \rangle \cong T^2, \tag{4.3b}$$

$$\langle \omega_A^4 \rangle = (K/m)^2, \tag{4.3c}$$

$$\langle \omega_B^4 \rangle \cong T^2, \tag{4.3d}$$

$$\langle \omega_C^2 \rangle = 4K/3m, \tag{4.4a}$$

and

$$\langle \omega_C^4 \rangle = \tfrac{16}{3}(K/m)^2. \tag{4.4b}$$

Consequently, as $T \rightarrow 0$, $R_A \rightarrow 1$, $R_B \rightarrow \infty$, and $R_C \rightarrow \sqrt{3}$. We therefore find that in low-temperature limit $(T \rightarrow 0)$, the variables B_n, which are finite at the potential minimum, give $R \rightarrow \infty$, while those that go to zero lead to a finite value for R. In addition, if the secular variables are like the A_n's i.e., they are simple numerical multiples of a coordinate that in the Hamiltonian plays the role of a harmonic-oscillator coordinate, then the corresponding $R \rightarrow 1$. As summarized at the end of the previous section, for $R = 1$, the entire amplitude of the spectral function belongs to the oscillator (i.e., $X = 1$). Since $\delta = 1$ the resonance is at $\omega = \pm \langle \omega^2 \rangle^{1/2}$, which is given by K/m. The oscillator width $\gamma = 0$. At the other extreme, for $R \rightarrow \infty$ the entire amplitude is in the central peak (i.e., $A = 1$) and it has vanishing width. Thus, it is the unity in the variable B_n, which expresses no dynamics, that gives rise to

the zero-frequency, zero-width peak. Since this result is obtained in a harmonic potential, it is not related to inter-valley dynamics. Associating such central peaks exclusively with intervalley transitions[5] is therefore incorrect.

V. EFFECT OF ROTATION-TRANSLATION COUPLING ON THE ORIENTATIONAL DYNAMICS

In the numerical calculations presented in Sec. IV, we assumed that the rotational dynamics took place in the potential $V_0(\theta,\phi)$ produced by the rigid-ion cage. One of the important characteristics of molecular impurities in ionic crystals is the coupling between orientational and translational degrees of freedom given by H_{TR} [see Eq. (2.4)]. The effect of H_{TR} on rotational dynamics can appear through three quantities, the isothermal susceptibility χ_T, the frequency scale ω_0, and R. The effect of H_{TR} on χ_T can be easily studied by removing H_{TR} by a canonical transformation which leads to a modification of the rigid ion-cage potential V_0 by a self-energy contribution V_s, i.e.,[12,13]

$$V_0(\theta,\phi) \rightarrow V(\theta,\phi) = V_0(\theta,\phi) + V_s(\theta,\phi) , \tag{5.1}$$

where

$$V_s(\theta,\phi) = \tfrac{1}{2} \sum_{\alpha=1}^{5} D_\alpha \mid Y_\alpha(\theta,\phi) \mid^2 \tag{5.2}$$

and

$$D_\alpha = -2 \sum_{j,\mathbf{k}} \frac{\mid V_{\alpha j}(\mathbf{k}) \mid^2}{\hbar \omega_{j,\mathbf{k}}} . \tag{5.3}$$

The rotation-phonon coupling constants $V_{\alpha j}(\mathbf{k})$ between the orientational variable $Y_\alpha(\mathbf{k})$ and phonons of mode j and wave vector $\mathbf{k}$ are given in Eq. (2.9). For cubic symmetry, $D_1 = D_2 = D_{e_g}$ and $D_3 = D_4 = D_5 = D_{t_{2g}}$. For this case the self-energy contribution to the potential is given by

$$V_s(\theta,\phi) = (15/16\pi)(D_{e_g} - D_{t_{2g}})Q(\theta,\phi) , \tag{5.4}$$

where $Q(\theta,\phi)$ is the Devonshire potential,

$$Q(\theta,\phi) = \sin^4\theta \, (\sin^4\phi + \cos^4\phi) + \cos^4\theta . \tag{5.5}$$

The effect of H_{TR} on $\langle \omega^2 \rangle$ and R has to be calculated explicitly. In the calculation that follows we ignore the explicit dynamics of the phonon variables. The additional torque produced by H_{TR} on the rotor dynamics is averaged over phonon coordinates using a canonical transformation to eliminate H_{TR} while taking the trace over phonon coordinates.

We find that H_{TR} has two effects on the calculation of moments. First, as in the case of χ_T, the rigid-lattice potential $V_0(\theta,\phi)$ is replaced by $V_0(\theta,\phi) + V_s(\theta,\phi)$ and this indirectly alters the values of $\langle \omega^2 \rangle, \langle \omega^4 \rangle$ at a given T by modifying the cubic potential in which the molecule rotates through the Boltzmann factor (see Appendix). Also, there is a new contribution to $\langle \omega^4 \rangle$, but not to $\langle \omega^2 \rangle$, that comes from an additional torque that acts on the molecule resulting from nonzero values of D_{e_g} and $D_{t_{2g}}$. Thus, H_{TR} can potentially alter the nature of the orientational dynamics beyond a simple change in the single-site potential from $V_0(\theta,\phi)$ to $V(\theta,\phi)$. Because of this we briefly summarize the details of our calculation. In the presence of H_{TR},

$$\dot{U} = \{U,H\} = \{U,H_R\} \tag{5.6}$$

and only H_R contributes to $\dot{U}$. Both $\langle \dot{U},\dot{U} \rangle$ and $\langle U,U \rangle$ can be calculated after removing H_{TR} by a canonical transformation, and we find that

$$\langle \dot{U},\dot{U} \rangle = \mathrm{Tr}(e^{-\beta \tilde{H}_R} \dot{U}\dot{U})/\mathrm{Tr}\, e^{-\beta \tilde{H}_R} \tag{5.7}$$

and

$$\langle U,U \rangle = \mathrm{Tr}(e^{-\beta \tilde{H}_R} UU)/\mathrm{Tr}\, e^{-\beta \tilde{H}_R} , \tag{5.8}$$

where

$$\tilde{H}_R = H_R + V_s(\theta,\phi) . \tag{5.9}$$

In the calculation of $\ddot{U} = \{\dot{U},H\}$, we find that

$$\ddot{U} = \ddot{U}_1 + \ddot{U}_2 \equiv \{\dot{U},H_R\} + \{\dot{U},H_{TR}\} . \tag{5.10}$$

For $U = Y_\alpha(\theta,\phi)$, the second contribution $\ddot{U}_2$ in Eq. (5.10) is found to be

$$\ddot{U}_2 = -\frac{1}{I} \left[\frac{\partial Y_\alpha}{\partial \theta} \sum_\beta \frac{\partial Y_\beta}{\partial \theta} + \frac{1}{\sin^2\theta} \frac{\partial Y_\alpha}{\partial \phi} \sum_\beta \frac{\partial Y_\beta}{\partial \phi} \right] \hat{b}_\beta , \tag{5.11}$$

where $\hat{b}_\beta$ is an operator in the phonon space:

$$\hat{b}_\beta = \sum_{j,\mathbf{k}} V_{\beta j}(\mathbf{k})(b_{j,\mathbf{k}} + b_{j,-\mathbf{k}}^\dagger) .$$

Since $\langle \omega^4 \rangle$ can be written in the form

$$\langle \omega^4 \rangle = -\frac{1}{\beta} \frac{\langle \{\ddot{U},\dot{U}\} \rangle}{\langle U,U \rangle} ,$$

it is apparent that this also splits into two contributions, $\langle \omega_c^4 \rangle$ and $\langle \omega_{nc}^4 \rangle$, where $\langle \omega_c^4 \rangle$ is calculated using the formulas in the Appendix with $V = V_0 + V_s$ and

$$\langle \omega_{nc}^4 \rangle_\alpha = -\frac{1}{\langle Y_\alpha^2 \rangle} \frac{1}{\beta I^2} \sum_\beta D_\beta \left\langle \left[\frac{\partial Y_\alpha}{\partial \theta} \right]^2 \left[\frac{\partial Y_\beta}{\partial \phi} \right]^2 + \frac{2}{\sin^2\theta} \frac{\partial Y_\alpha}{\partial \theta} \frac{\partial Y_\alpha}{\partial \phi} \frac{\partial Y_\beta}{\partial \theta} \frac{\partial Y_\beta}{\partial \phi} + \frac{1}{\sin^4\theta} \left[\frac{\partial Y_\alpha}{\partial \phi} \right]^2 \left[\frac{\partial Y_\beta}{\partial \phi} \right]^2 \right\rangle , \tag{5.12}$$

with D_β defined in Eq. (5.3). The thermal averages in the calculation of $\langle \omega_c^4 \rangle$ and $\langle \omega_{nc}^4 \rangle_\alpha$ have to be taken with respect to $\tilde{H}_R$ given in Eq. (5.9) and were identified as the cubic and noncubic components of the local distortion

in Ref. 10.

There is a similarity between the effect of H_{TR} on $\langle \omega^2 \rangle$ and $\langle \omega^4 \rangle$ and that of exchange interaction H_{ex} between spins that interact via dipole-dipole interaction. As is well

known[17] in magnetic resonance theories, H_{ex} modifies the fourth moment, keeping the second moment unchanged, the net result being an exchange narrowing of the spectral line shape. In our problem, however, there is an additional effect associated with the renormalization of the cubic potential in which the orientational dynamics takes place. The detailed study of the effect of H_{TR} on the spectral functions of T_{2g} and E_g symmetries will be presented in the next section.

VI. RESULTS AND DISCUSSION

A. Effective cubic potential

The rigid-cage potential was calculated by using the parameter values given in Table II. The values of hexadecapole moment (Q_4) and quadrupole moment (Q_2) of the $(CN)^-$ molecular ion were taken from the Table I of Le-Sar and Gordon.[18] To facilitate the calculation of the potential $V(\theta,\phi)$ and its derivatives which appear in the expressions for $\langle \omega^4 \rangle$ (see Appendix), we expand $V(\theta,\phi)$ in terms of the first six cubic harmonics following Fehlner and Vosko[19] and write it as

$$V(\theta,\phi) = \sum_{i,j} A_{i,j} Q^{i-1} S^{j-1} , \tag{6.1}$$

where Q has been defined in Eq. (5.5) and

$$S(\theta,\phi) = \sin^4\theta \cos^2\theta (1 - \sin^4\phi - \cos^4\phi)/2 .$$

It should be noted that repulsion contributes to all A_{ij}'s, whereas the hexadecapole moment contributes only to A_{21}. The dominant coefficients are A_{21} and A_{12} and the rest make small contributions to the total potential. The values of A_{21}'s and A_{12} are given in Table III, where we also give the self-energy contribution to A_{21} (see below).

The self-energy contribution to A_{21}, to be denoted as A_{21}^S, was obtained by using the parameters A_R and B_R of Sahu and Mahanti,[13] but a different set of values for A_Q and B_Q, the quadrupole—electric-field-gradient coupling contribution to the rotational-translational coupling. These are calculated by using a value of Q_2 given in Table II instead of -4.64×10^{-10} esu Å^2 used in Ref. 14. The values of coupling constants used in the present paper are $A_R = 4379$, $B_R = -988$, $A_Q = -3954$, and $B_Q = 3225$, all in units of K/Å. In the calculation of rotational-translation coupling coefficients $v_{\alpha\mu}(\mathbf{k})$ of Eq. (2.9), we have included contributions up to third-nearest neighbor. The phonon frequencies $\omega_{j\mathbf{k}}$ and corresponding polarization vectors were calculated within a rigid-ion model, and the Brillouin-zone sums were carried out by using the special-point method.[20] The self-energy parameters D_{e_g}

and $D_{t_{2g}}$ are found to be -985 and -3743 K, respectively. Using the following definition for A_{21}^S, the self-energy contribution to A_{21},

$$A_{21}^S = \tfrac{15}{16}(D_{e_g} - D_{t_{2g}}) , \tag{6.2}$$

we find A_{21}^S equal to 823 K (see Table III). The effect of D_{e_g} and $D_{t_{2g}}$ on $\langle \omega^4 \rangle$ will be discussed later in this section. Before that we would like to discuss the importance of the self-energy contribution to the single-site potential.

If we consider A_{21}^R, i.e., only the repulsion contribution to $V(\theta,\phi)$, then the minima are along [111] and equivalent directions, and the barrier height Δ is about 340 K. Inclusion of the hexadecapole contribution A_{21}^H to A_{21} shifts the minima to the [100] and equivalent directions and gives $\Delta \cong 650$ K. The self-energy contribution A_{21}^S is not large enough to shift the minima back to [111], but does reduce the barrier height to 250 K. Experimentally, the barrier heights have been found to be much smaller than these numbers, i.e., they are of the order of 50—100 K. Also for $(CN)^-$ in KCl and KBr, the minima are along the [111] directions. Because of the cancellation between two large numbers A_{21}^R and A_{21}^H, a small change in one will alter the nature of the single-site potential drastically. In the present study, we change $V(\theta,\phi)$ by changing A_{21}^H, which is equivalent to modifying the $(CN)^-$ hexadecapole moment. We define a parameter r, such that $A_{21}^H \to r A_{21}^H$, and vary r. The values of $V(\theta,\phi)$ with the self-energy contribution for the [100], [110], and [111] directions for $0.6 \leq r \leq 1$ are given in Table IV, where minima are denoted by footnote a and Δ is the height of the lowest energy barrier.

B. Central peak weight and spectral function

We will discuss the effect of translation-rotation coupling (TRC) on the orientational dynamics in several steps. First, we choose a particular temperature and study how the central-peak weight (A) changes when TRC is included. Next, we discuss the temperature dependence of A for two suitably chosen values of r, which determines the strength of the molecular hexadecapole moment.

In Figs. 3(a), 3(b), and 3(c), we show the effect of TRC on A for E_g and T_{2g} symmetries in three stages. The temperature was chosen to be 50 K, which is an intermediate temperature, i.e., $k_B T \sim \Delta$, Δ being the height of the potential barrier. In Fig. 3(a), the effect of TRC is in-

TABLE III. Various contributions to the expansion coefficients A_{ij} of the single-site potential $V(\theta,\phi)$ [see Eq. (6.1)] expressed in units of K. The magnitudes of the rest of the coefficients are less than 10 K.

A_{12}^R	A_{21}^R	A_{21}^H	A_{21}^S	A_{22}^R	A_{31}^R
1731	2351	-3765	823	56	68

TABLE IV. Single-site potential for three different symmetry directions for different values of hexadecapole-moment (Q_4) reduction factor r. $Q_4 \to r Q_4^0$, where Q_4^0 is the free-ion value. All entries are in units of K.

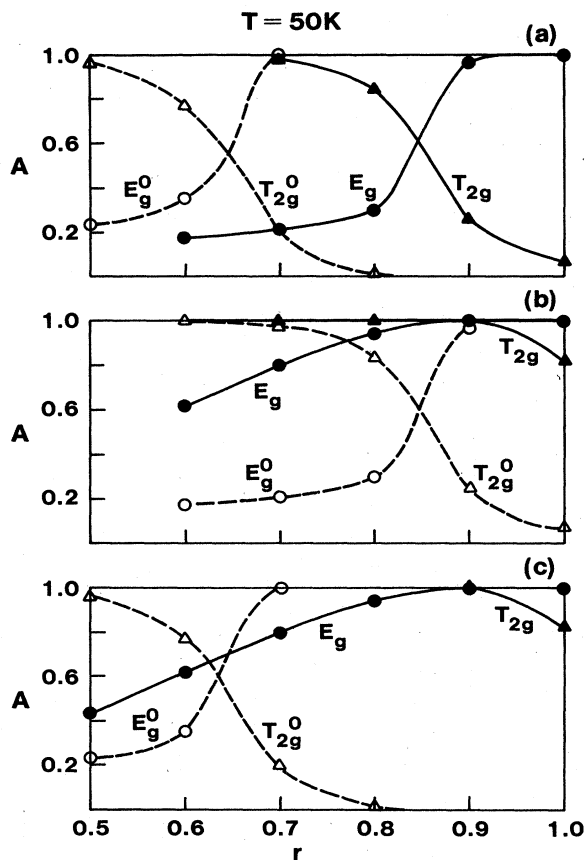| r	$V[100]$	$V[110]$	$V[111]$	Δ
0.6	985	475	378[a]	97
0.7	608	287	252[a]	35
0.8	232	98[a]	127	29
0.9	-145[a]	-90	1	55
1.0	-521[a]	-278	-124	243

[a]The minimum of the potential.

FIG. 3. Strength of central peak A as a function of r, defined in Table IV at $T = 50$ K. (a) Dashed lines—without TRC; solid lines—TRC incorporated only by the self-energy ($V = V_0 + V_s$). (b) Dashed lines—TRC incorporated only by the self-energy; solid lines—TRC incorporated by both the self-energy and the fourth moment. (c) Dashed lines—without TRC; solid lines—TRC incorporated by both the self-energy and the fourth moment.

corporated through a modification of the single-site potential V, as given in Eq. (5.1). V_s not only changes various thermal averages through the Boltzmann factor, but also the fourth moment $\langle \omega^4 \rangle$ [see Eq. (5.1)].

A rather drastic change in the values of A_{E_g} and A_{2T_g} occurs upon inclusion of the self-energy in the potential energy. This arises from the tendency of the potential minimum to shift from the [100] direction to the [111] direction. The point where $A_{E_g} = A_{2T_g}$ shifts from $r = 0.65$ to $r = 0.85$. At $r = 0.75$ in the absence of the self-energy $A_{E_g} \simeq 1$ and $A_{T_{2g}} \simeq 0.06$. In the presence of the self-energy, $A_{E_g} = 0.24$ and $A_{T_{2g}} = 0.94$.

In Fig. 3(b), we show how A changes when the new contribution to $\langle \omega^4 \rangle$ coming from TRC [see Eq. (5.12)], denoted by $\langle \omega_{nc}^4 \rangle$, is included in the calculation of spectral weight. The single-site potential $V = V_0 + V_s$ is the same for both the dashed and the solid curves of this figure. The major effect of $\langle \omega_{nc}^4 \rangle$ is an overall enhancement of A for all values of r. The effect is dramatic for the values of r at which the potential barrier height Δ is small, i.e., near the E_g-T_{2g} crossover region. The crossover point shifts by a very small amount to a higher value of r, which is perhaps due to the detailed nature of the potential.

In Fig. 3(c), we show the entire effect of TRC on A. The dashed curves are those of Fig. 3(a) and the solid curves are those of Fig. 3(b). TRC changes A dramatically and should be incorporated in a proper theoretical understanding of the orientational dynamics of molecular ions. The nonrigid nature of the ion cage surrounding a molecular impurity in alkali halides strongly alters the latter's dynamics due to a strong coupling between the rotational and translational dynamics. We believe, however, that the present calculation overestimates the effect of the nonrigid cage. If ω_{rot}, the characteristic rotational frequency, is much larger than ω_{vib}, the characteristic frequency of the cage dynamics, then the cage will not respond to the rotational dynamics. Consequently, the
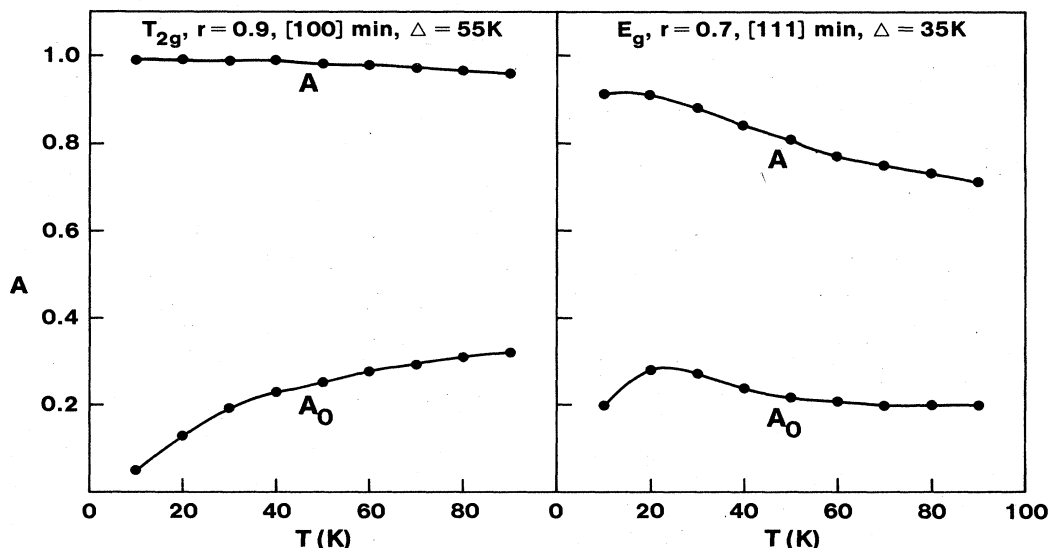

FIG. 4. Temperature dependence of the strength of the central peak without TRC (A_0) and with the full effect of TRC (A).

orientational motion will primarily take place in a rigid, although possibly noncubic, cage. Thus, a proper theory should include the cage dynamics explicitly. Within the Mori approach, we have to go beyond $\langle \omega^4 \rangle$ in the calculation of orientational relaxation function.

In Figs. 4(a) and 4(b), we present our results for the central-peak enhancement for different temperatures. At very low temperatures $T \leq 10$ K, the numerical results are not reliable and one needs to study the low-T ($T \rightarrow 0$ K) behavior of $\langle \omega^4 \rangle$ and $\langle \omega_{nc}^4 \rangle$ analytically. For physical systems, however, one expects the quantum behavior to be important and the $T \rightarrow 0$ K limit of a classical theory to be only of academic importance. We have not, therefore, pursued the analytical studies in great detail.

C. Comparison with experiment and discussion

For the KBr-CN⁻ system, Callender and Pershan[1] found that at low temperatures ($T \leq 100$ K) the E_g spectrum showed a librational peak, whereas the T_{2g} spectrum showed a central peak (referred to as relaxational peak by de Raedt and Michel[5]). From Table IV of the present paper, we see that for the KBr-CN⁻ system, the single-site potential has a [111] minimum when the self-energy contribution V_s to the single-site potential is included and the free-ion hexadecapole moment is reduced to about 60—70 % of its free-ion value. The barrier height Δ is between 97 and 35 K, which is a reasonable value for this system. It should be emphasized that the shallow barrier height is a result of strong rotation-translation coupling, i.e., large V_s.

If we treat the single-site potential $V = V_0 + V_s$ as an effective rigid potential in which the CN⁻ molecules rotate, then the E_g and T_{2g} spectral functions will be in excellent agreement with experiment. For example, see Fig. 3(a), where for $r = 0.7$ the solid curve shows dominant E_{2g}-librational and T_{2g}-relaxational response. However, the strong rotation-translation coupling which modifies the bare single-site potential V_0 also alters the orientational dynamics [see Eq. (5.12)] explicitly by changing the fourth moment. This latter modification is so strong that for $r = 0.6, 0.7$, both the E_g and T_{2g} spectral functions show dominant central-peak or relaxational response [see Fig. 3(c)]. This is in disagreement with the experiment. We therefore conclude that the apparent agreement between experiment and the theory using an effective rigid potential is fortuitous. Whether an improved treatment of the orientational dynamics by including the explicit effects of translational dynamics will restore the agreement between theory and experiment remains to be seen.

In summary, we believe that in these systems where there is a strong coupling between the rotational and translational degrees of freedom, a proper theory of orientational dynamics should include the translational dynamics. In the calculation of rotational relaxation functions within Mori's continued fraction scheme, one has to go at least up to $\langle \omega^6 \rangle$, the sixth moment. Before applying this improved theory to real systems, one has to test it for simple-model systems first.

APPENDIX

The formulas needed to evaluate $\langle \omega^2 \rangle$ and $\langle \omega^4 \rangle$ in a rigid cubic potential were given by de Raedt and Michel[5] for the E_g and T_{2g} symmetries for $l = 2$. Although our formulas for $\langle \omega^2 \rangle$ agree, they have a different form for $\langle \omega^4 \rangle$. We have for the $\langle \omega^4 \rangle$

$$\langle \omega^4 \rangle_{E_g} = \frac{\frac{48}{\beta^2 I^2}(1 + 3\langle \cos^4\theta \rangle) + \frac{9}{\beta I^2}\left\langle \sin(2\theta)\frac{\partial}{\partial\theta}\left[\sin(2\theta)\frac{\partial V}{\partial\theta}\right]\right\rangle}{9\langle \cos^4\theta \rangle - 1}, \tag{A1}$$

$$\langle \omega^4 \rangle_{T_{2g}} = \frac{48}{\beta^2 I^2}\frac{1 - \langle \cos^4\theta \rangle}{1 - \langle 3\cos^4\theta \rangle}$$

$$+ \frac{3}{\beta I^2}\frac{\left\langle \cos^2 2\theta\frac{\partial^2 V}{\partial\theta^2}\right\rangle + \left\langle \cot^2\theta\frac{\partial^2 V}{\partial\phi^2}\right\rangle - \left\langle \frac{\partial V}{\partial\theta}(1 - 2\cos^2\theta)\cot\theta\right\rangle + \left\langle \frac{\partial V}{\partial\theta}\frac{\partial}{\partial\theta}(\sin^4\theta + \cos^4\theta)\right\rangle}{1 - 3\langle \cos^4\theta \rangle)}. \tag{A2}$$

[1] R. Callender and P. S. Pershan, Phys. Rev. A **2**, 672 (1970).
[2] D. Fontaine and H. Poulet, Phys. Status Solidi B **58**, K9 (1973).
[3] H. V. Beyeler, R. Bauman, and W. Känzig, Phys. Kondens. Mater. **11**, 286 (1970).
[4] V. Naraynamurty and R. O. Pohl, Rev. Mod. Phys. **42**, 201 (1970).

[5] B. de Raedt and K. H. Michel, Phys. Rev. B **19**, 767 (1979).
[6] F. Lütty, in *Defects in Insulating Crystals,* proceedings of the International Conference on Defects in Insulating Crystals, Riga, 1981, edited by V. M. Turkevich and K. K. Shvarts (Springer, Berlin, 1981), pp. 69—89.
[7] F. Lüty and J. Ortiz-Lopez, Phys. Rev. Lett. **50**, 1289 (1983).

[8]K. H. Michel and J. M. Rowe, Phys. Rev. B **22**, 1417 (1980).

[9]C. G. Kuper and G. D. Whitfield, *Polarons and Excitons* (Oliver and Boyd, Edinburgh, 1963).

[10]S. D. Mahanti and G. Kemeny, Phys. Rev. B **30**, 7362 (1984).

[11]K. H. Michel and J. Naudts, Phys. Rev. Lett. **39**, 212 (1977); J. Chem. Phys. **67**, 547 (1977).

[12]B. de Raedt, K. Binder, and K. H. Michel, J. Chem. Phys. **75**, 2977 (1981).

[13]D. Sahu and S. D. Mahanti, Phys. Rev. B **29**, 340 (1984).

[14]D. Sahu and S. D. Mahanti, Phys. Rev. B **26**, 2981 (1982).

[15]D. Sahu, Ph. D. thesis, Michigan State University, 1983.

[16]H. de Raedt and B. de Raedt, Phys. Rev. B **15**, 5379 (1977).

[17]C. P. Slichter, *Principles of Magnetic Resonance* (Harper and Row, New York, 1963), p. 112.

[18]R. LeSar and R. G. Gordon, J. Chem. Phys. **77**, 3682 (1982).

[19]W. R. Fehlner and S. H. Vosko, Can. J. Phys. **54**, 2159 (1976).

[20]A. Bansil, Solid State Commun. **16**, 885 (1975).